

Received December 14, 2018, accepted January 14, 2019, date of publication January 29, 2019, date of current version February 20, 2019.

Digital Object Identifier 10.1109/ACCESS.2019.2895904

Highly Efficient Unpackaged 60 GHz Planar Antenna Array

YAZAN AL-ALEM¹ (Student Member, IEEE), AND AHMED A. KISHK¹ (Fellow, IEEE)

Department of Electrical and Computer Engineering, Concordia University, Montreal, QC H3G 1M8, Canada

Corresponding author: Yazan Al-Alem (y_alalem@encs.concordia.ca)

ABSTRACT A high gain antenna array is designed and fabricated at 60 GHz. The array is via-less and made on a single dielectric substrate. It can be easily integrated with millimeter wave transceivers. Very good agreement between the measured and simulated results is achieved. The array has 22.5 dBi gain with a maximum efficiency of 93% and a 3.2 % bandwidth.

INDEX TERMS High gain antenna array, millimeter-wave antenna array, low profile antenna, planar antenna.

I. INTRODUCTION

Recently, there has been an increasing interest in high gain antennas at millimeter-wave frequencies. A high gain antenna is an essential component for any millimeter-wave transceiver system, where such high gain antenna plays a vital role in compensating the high path loss encountered at such frequencies [1], [2]. In the literature, various methods were employed to design high gain antennas at millimeter-wave frequencies [3]–[9]. In [8], an active microstrip antenna integrated with a three-stage pseudomorphic high electron mobility transistor amplifier was designed. Such an active antenna design is suitable for narrowband wireless local and personal area networks (WLAN/WPAN) applications. However, it demands a considerable amount of power consumption, which can constitute some limitations for mobile devices. In [7], a high gain array was comprised of radiating slots that are fed through a substrate integrated waveguide (SIW) power divider network. Such a design is very robust in terms of its radiation characteristics because of the SIW feeding network, which is sufficiently shielded/package type of feeding networks [10]. In [11], a 60 GHz antenna array with a dual-resonant slot-patch antenna was designed using LTCC technology. The shrinking effect of the LTCC substrates makes it more challenging and expensive in terms of its fabrication process. In [12], a monolithic polymer-based high gain Dielectric Resonator Antenna (DRA) was implemented efficiently. In [13] a wideband magneto electric dipole antenna was designed, despite the high bandwidth

feature of magneto-electric dipoles, they are still not known for being low profile. In [14] and [15], printed dipole antennas were designed at 30 GHz using printed circuit board technology, the element radiation pattern is an end-fire, and would still be limited to linear array configurations. In [16] and [17], SIW fed 60 GHz antennas were implemented. In [18], LTCC type of structure was implemented at 60 GHz, the LTCC technology is well suited for a high level of integration, and can push down the size of the structure effectively. However, it is still expensive, and more demanding in terms of the fabrication process due to the shrinking effect. In [19], a broadband 60 GHz slot antenna was designed. The bandwidth of the antenna was optimized using a cavity underneath the antenna. The EBG feeding provides reasonable efficiency and good shielding mechanism. However, the antenna gain was compromised in this work. In [20], 60 GHz on-chip antenna using “IPD” integrated passive device process was implemented. Such a process provides a high level of integration. On-chip designs are known for their low efficiencies due to the silicon substrate, in this IPD process, the efficiency was improved by using a glass substrate. In [21], a 60-GHz end-fire fan-like antenna with a wide beam-width was implemented, the wide beam-width reflects a relatively lower gain. Another technique to implement high gain antennas is the use of superstrates to increase the antenna gain. However, superstrates usually make the antenna very obtrusive and bulky [6], [22]–[34]. Most of these solutions require multiple substrates and through-hole vias which increase the cost and complexity of the antenna structure. In this paper, a low-cost single substrate (via-less), high gain, and efficient antenna array structure is proposed.

The associate editor coordinating the review of this manuscript and approving it for publication was Mingjian Li.

The authors had previously designed an antenna element that utilizes the microstrip line discontinuity radiation in a constructive way to create an efficient high gain antenna [5]. The structure only used a single dielectric substrate that eases the manufacturability and hence reduces the cost. Also, as the element structure can be perceived as being comprised of four magnetic current elements, the element can be employed in a linear antenna array with a center to center separation between the elements greater than a free space wavelength with suppressed grating lobes [5]. Such feature of the antenna element can significantly relax the design of the array feeding network. In the previous work [5], a linear antenna array fed by a parallel microstrip feeding network was implemented at 60 GHz. However, the open microstrip line feeding network suffered from significant radiation losses. Here, we investigate the design of a 4x4 high gain antenna array with an efficient feeding network. Where we show that the element proposed in [5] is highly efficient and can be used in several planar array configurations such as series and parallel feeding networks and their combination in a way that even the feeding network does not provide significant losses as one is expecting at these frequencies.

The rest of the manuscript is organized as follows; Section II studies several feeding networks configurations and compares EBG packaged feeding networks with open/unpackaged feeding networks, section III discusses the proposed antenna array structure and experimental prototyping results, section IV concludes this work and discusses potential future work.

II. ARRAY FEEDING NETWORK STUD

At millimeter-wave frequencies, having a packaged guiding structure is highly desirable to eliminate any possible radiation losses that reduce the antenna efficiency and affect the radiation characteristic of the antenna. Hence, it maintains the radiation characteristics of the antenna only. Packaging, or shielding, in other words, is usually done by surrounding the feeding structure by a metal surface. For a planar feeding network, this can be done by shielding the feeding network from the top and bottom by metal sheets. Such a method is good for suppressing the radiation from the feeding network. However, such method is undesirable due to the excitation of parallel plate waveguide modes within the shielded package, which eventually constitute a significant source of losses in the feeding structure. Ridge gap waveguide is an example of a new technology that treats such a problem and prevents the propagation of parallel plate waveguide modes [35]. Ridge gap waveguide employs electromagnetic bandgap (EBG) periodic structures, such as Sievenpiper mushroom cells [36], to create the EBG.

Fig. 1-a shows the geometry and parameters of a unit cell of the periodic structure. Fig. 1-b shows its corresponding two-dimensional dispersion diagram covering the irreducible Brillouin zone of the cell. The cell is designed to provide the EBG centered at 60 GHz with a bandwidth of 26 GHz (i.e., from 50 to 76 GHz). In [35], a printed ridge gap

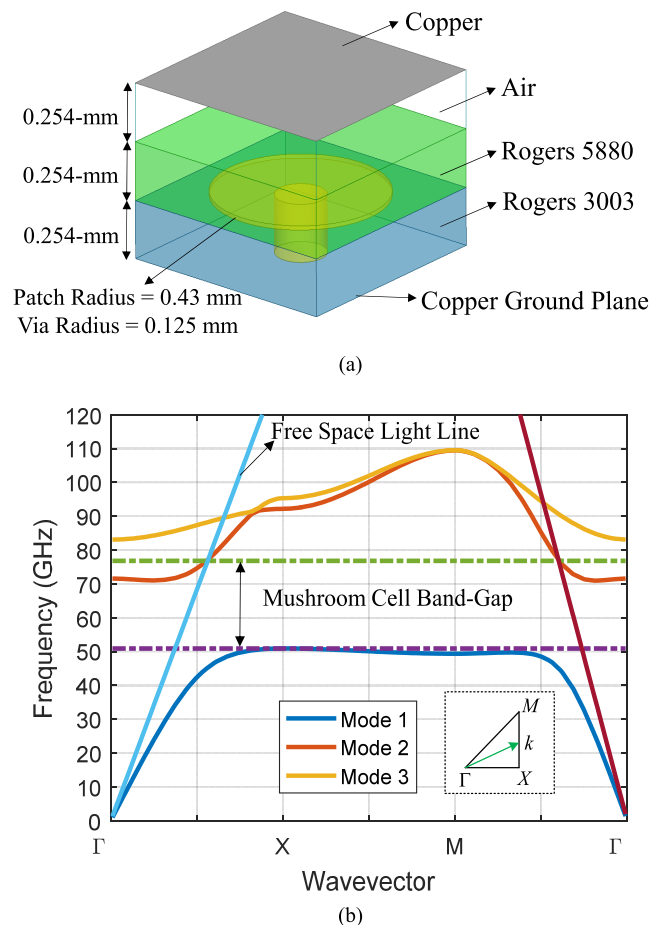


FIGURE 1. (a) EBG mushroom cell dimensions. (b) Dispersion diagram of the Sievenpiper mushroom cell.

waveguide (PRGW) with facilitated design properties is proposed. In [37], a similar concept was implemented using a classical ridge gap waveguide and was referred to as an inverted microstrip line. The PRGW in [35], facilitates the design procedure because the guideline lies in a separate layer without a need of plated vias (different level from the textured periodic surface). As such, curved lines can be designed easily once compared to the classical RGW, where the guideline is located on the same surface of the mushroom patches and must be grounded by conducting vias. A detailed discussion of the pros of the structure is provided in [35].

Fig. 2-a shows a section of the printed ridge gap waveguide Fig.2-b shows its corresponding dispersion diagram. A Quasi-TEM mode is excited as expected within the bandgap. A feature of the ridge gap structure is that the guiding bandwidth is a little less than the cell bandgap [35].

Fig. 3 shows the complete structure of the PRGW antenna array. The elements are arranged to provide boresight radiation by differentially feeding each pair; such arrangement reduces the cross-polarization level significantly. As shown in Fig. 3. The left and right side of the array are combined with the PRGW power combiner. Such a packaged solution prevents radiation from this part (power combiner/divider)

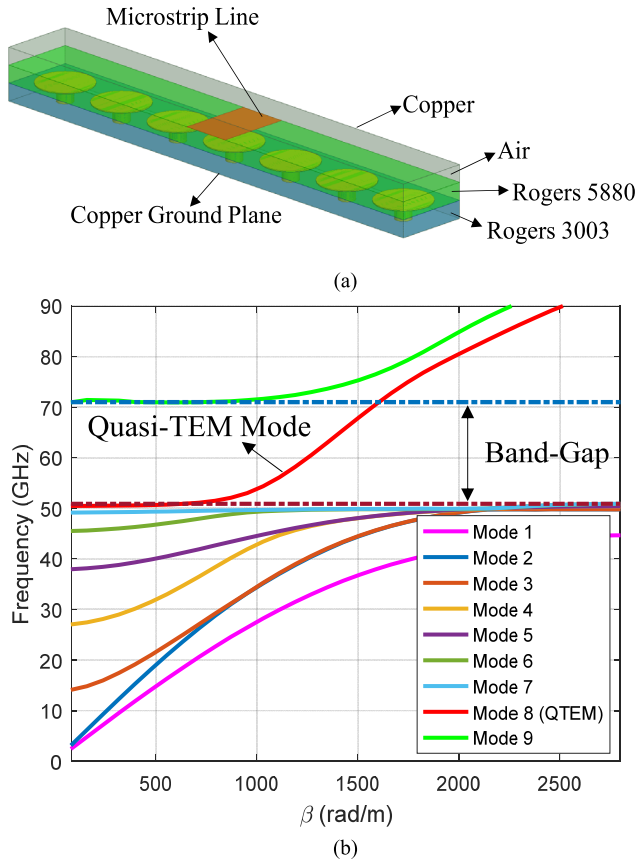


FIGURE 2. (a) Printed ridge-gap air microstrip line. (b) Printed ridge-gap air microstrip line dispersion diagram.

and any interference with the radiating array. It should be stated that the line widths of the power combiner/divider are different from those of the open microstrip lines, but with the same characteristic impedances.

The second feeding network is the same as the above, but its power combiner is made entirely from the same conventional microstrip line feeding the array. Therefore, all the feeding network is an unpackaged open microstrip line network. As the radiating elements portion is identical in the two cases, and by guaranteeing that the two structures have equally appropriate matching levels at the main feeding point, the difference in the efficiency of the two structures indicates the losses level of the feeding network. Since the same type of material is used in both designs, it can be inferred that conduction and dielectric losses are the same. On the other hand, it is well known that packaged PRGW feeding eliminates both surface-waves and radiation losses. However, in open microstrip line technology, such losses can't be avoided. Therefore, studying the PRGW solution is essential to have a reference point regarding the losses attributed to radiation and surface-waves from the feeding network of an open structure. Similar to the PRGW structure, the packaged structure is shown in Fig.4. In this case, the feeding network is covered with a mushroom cell layer acting as an AMC (Artificial Magnetic Conductor). The cell size is redesigned with the dimensions shown to operate

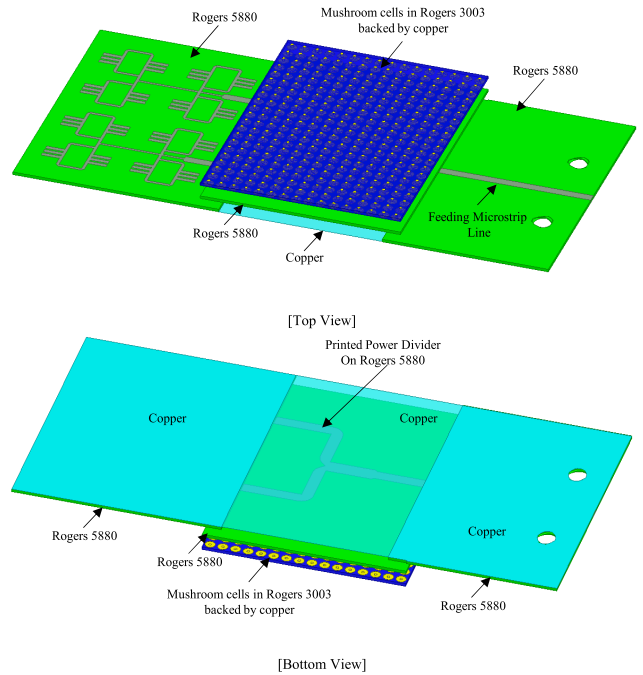
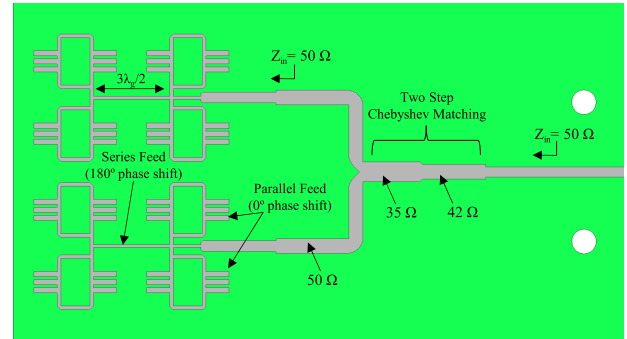


FIGURE 3. Antenna array fed by PRGW power divider.

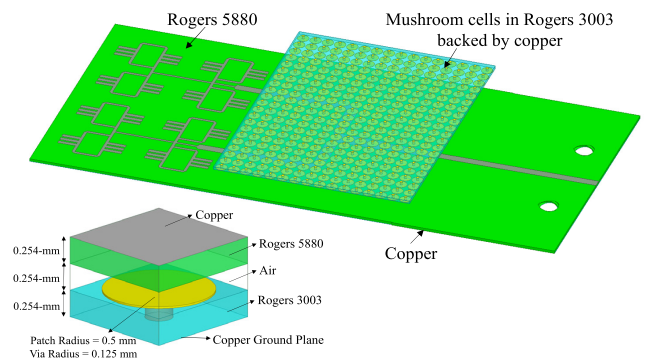


FIGURE 4. Antenna array fed by packaged microstrip line power divider.

within the required band. The signal propagates in the air in the PRGW, but it propagates in the dielectric substrate in the packaged solution. Therefore, a higher level of losses is expected in the packaged case due to the dielectric losses. Another difference in the packaged solution is that the signal propagates in the same substrate. Hence, the change in the width of the line is very negligible once compared with the

TABLE 1. Line width for different characteristic impedances.

Z_0	MSL	PRGW	Packaged
35 Ω	1.3 mm	1.7 mm	1.3 mm
42 Ω	1 mm	1.4 mm	1 mm
50 Ω	0.78 mm	1.05 mm	0.78 mm

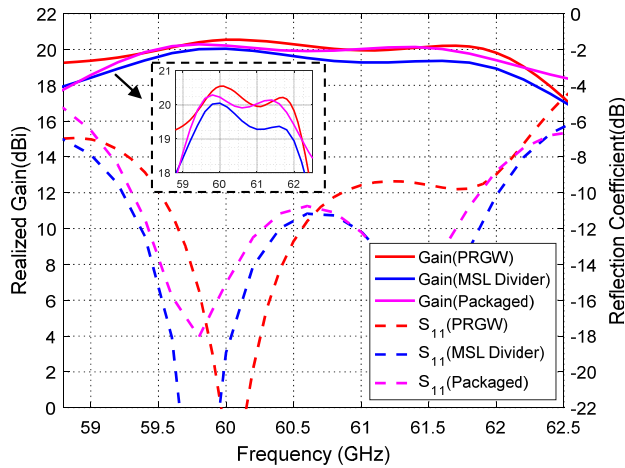


FIGURE 5. Realized gain and reflection coefficient for the proposed cases.

conventional open MSL case. Table 1 shows the line widths at 60 GHz for the proposed cases.

As shown in the array structure, two elements are fed in parallel, and the other combined two elements are fed in series. The length of the series feed is $1.5\lambda_g$. This length maintains 180° phase shift between the feed points. The 180° phase shift at the feed is required to counter the effect of physically flipping the element 180° . Also, the $1.5\lambda_g$ feed maintains one free-space wavelength between the elements. It is clear that the radiating element possesses a high directive nature that allows relaxing the distance between the radiating elements and thus relaxing the feeding network design as well as suppress the grating lobe level. Details about the element characteristics can be found in [5]. It is worth mentioning that series fed always poses bandwidth restriction in terms of the radiation pattern stability, as the phase shift between elements vary with frequency and hence steer the main beam [22], [38], [39]. However, within a narrowband such effect can be ignored, which is in line with the proposed case.

Fig. 5 shows the matching bandwidth, and the corresponding realized gain for the three cases, a boresight gain of 20.5 dBi is achieved for the PRGW solution, and the corresponding 10 dB return loss matching bandwidth is almost 3.66% (i.e., 2.2 GHz). The narrow bandwidth is attributed to the high-quality factor and correspondingly narrow bandwidth of the radiating element [5]. The conventional unpackaged microstrip line power divider feeding network is lower in terms of its realized gain level once compared with the PRGW solution; this is expected and attributed to the radiation and surface-wave losses from the open MSL power divider. The packaged solution realized gain level lies

in-between the open and the PRGW cases. The packaged solution suffers from additional dielectric losses due to the propagation in the dielectric medium and not air as in the PRGW case. It is important to notice that at the higher frequencies in the band above 60 GHz, the PRGW has a lower level of matching, which deteriorates the realized gain level. Therefore, the comparison is fairly drawn only at the center frequency (60 GHz) where all the cases have sufficient matching level.

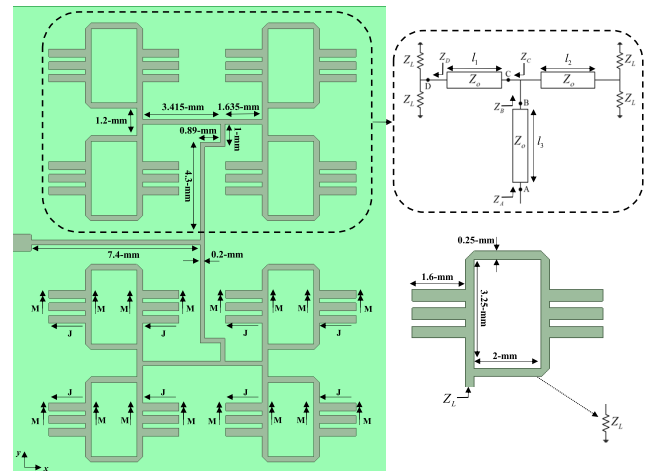


FIGURE 6. Antenna array with aggregated open microstrip line feeding network, (the distance from the center of the array to the end-lunch connector is the same for all cases. The feed line is only cropped in this figure).

PRGW as many packaged solutions necessitates the use of plated vias, those plated vias require a special process to be realized and consume considerable fabrication time. Therefore, the low cost and simplicity features of the open structure solution are obviously spotted once compared with PRGW or other packaged solutions (where it only needs a single substrate layer with no vias). This feature makes it even more desirable for integration purposes. This consequently raises the question, can open microstrip line technology be used with minimal compromise on efficiency and performance? In this work, the power divider is eliminated by aggregating all the elements of the configuration shown in Fig. 6. The typical procedure to design a feeding network for a 2D-array is by using power dividers and quarter wavelength transformers to match the parallel combination of the antenna elements to the desired system impedance. This procedure usually results in transmission lines with different characteristic impedances. Due to the limited space between the antenna array elements, the wide microstrip lines cannot be accommodated, especially in the aggregated configuration shown in Fig. 6. As an example, in Fig. 6 the width of the line that can fit between two radiating elements is constrained by the separation distance between them, such distance is fixed by the array design to reduce the grating lobes. Moreover, very wide microstrip lines can have significant radiation effects. Therefore, the feeding network design procedure proposed in Fig. 6 can provide the required matching impedance by

using any arbitrary characteristic impedance. As the procedure is illustrated in Fig. 6, and by the use of simple transmission line theory, the input impedance at point “A” will always be equal to Z_L as long all the lines (i.e., l_1 , l_2 , and l_3) are multiple of an odd integer of the guided quarter wavelength.

From Fig. 6, it is important to note that flipping the radiating elements along the y-axis does not require 180-degree phase shift feed to maintain boresight radiation; this is due to the fact that the currents can still run through the open stubs in the same direction as shown in Fig. 6. Also, the elevated distance feature provided by the elements in the E-plane (i.e., along the x-axis) [5], eases off the layout of the feeding lines between the radiating elements.

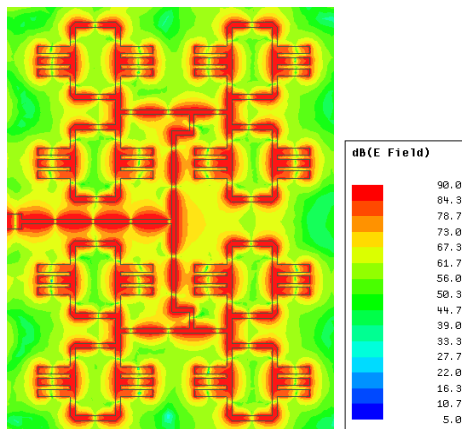


FIGURE 7. Electric field heat map for the aggregated open microstrip line fed antenna array at 60 GHz.

Fig. 7 shows the electric field heat map, a strong interaction between the feed lines and the antenna array elements due to their proximity is observed. Such strong interaction implies that the proper feeding structure of the array should be designed and tuned simultaneously with the presence of the antennas.

The aggregated proposed design in Fig. 6 is modular, where the dotted configuration can be reused and the array can be expanded and doubled easily. Very narrow lines can fit between the radiating elements easily as the matching procedure is independent of the characteristic impedance of the lines. Moreover, the proposed aggregated configuration can reduce the area of the whole array by almost half, where the area needed to accommodate the power dividers has been eliminated by embedding it between the elements. Hence, providing a more compact design. Fig. 8 shows the matching bandwidth of the array and the corresponding realized gain. As can be noticed, a 0.25 dBi gain enhancement is achieved over the open microstrip line power divider case. Such enhancement would be more significant with a larger array. The use of narrow lines reduces the bandwidth from 3.66% to 3.2%.

Fig. 9 shows the electric field heat map in the E-plane for the proposed structures, as can be observed the packaged cases have neat and stable radiation in the boresight direction.

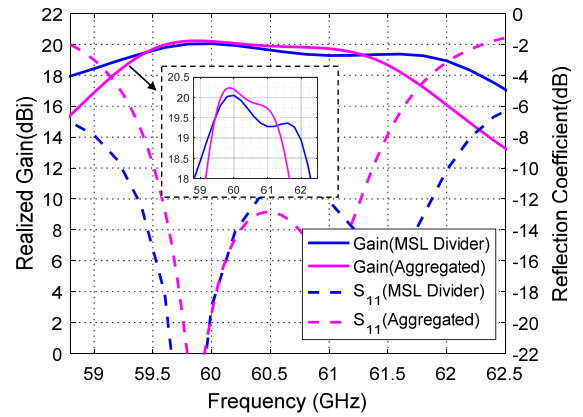


FIGURE 8. Realized gain and reflection coefficient for both open and aggregated fed microstrip line fed antenna arrays.

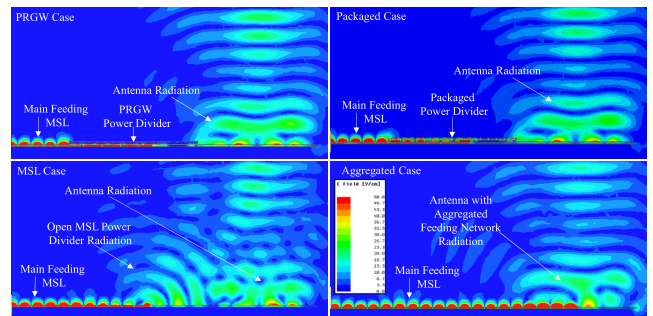


FIGURE 9. Electric field heat map in the E-plane for the proposed array structures.

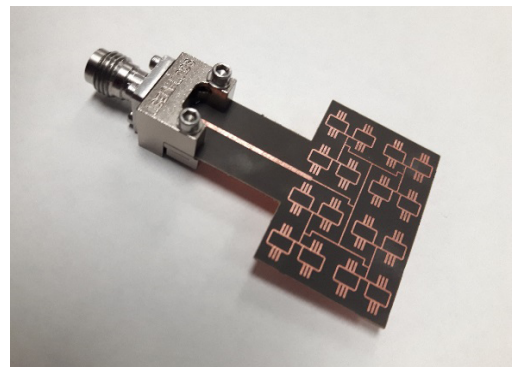


FIGURE 10. Proposed antenna array structure with aggregated microstrip feeding network.

The open MSL case suffers from the undesired power divider radiation; such radiation affects the radiation characteristics of the antenna array and the total gain and efficiency. The aggregated case resolves such issue, and have almost the same neat radiation characteristic as in the packaged case.

III. PROPOSED ANTENNA ARRAY

The study provided in the last section inspired the design of a high gain array that suits narrowband applications at 60 GHz. Even though the proposed aggregated feeding solution performance cannot fully match the PRGW solution, it still provides a low cost, efficient, and compact solution with minimal compromise on performance. Fig. 10 shows a photo of the

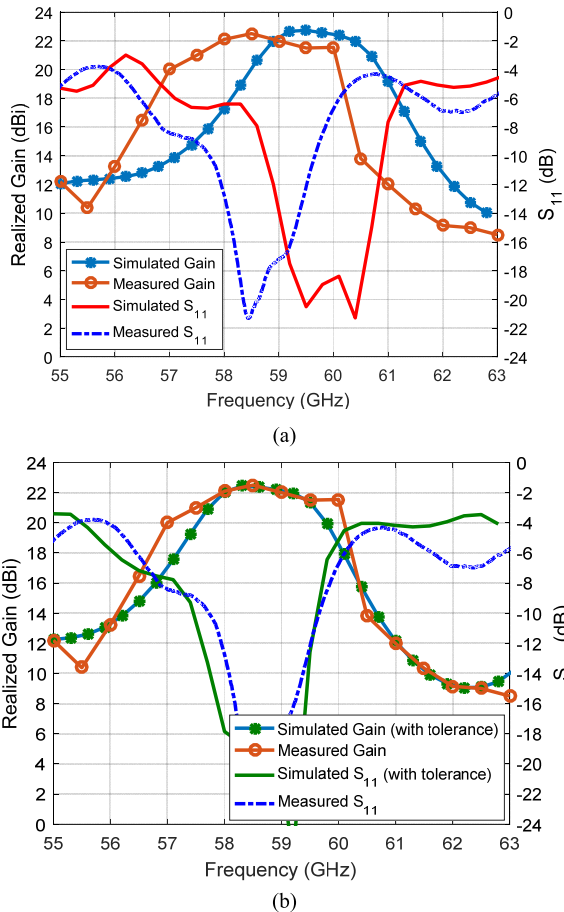


FIGURE 11. (a) Realized gain and reflection coefficient of the proposed antenna array. (b) Realized gain and reflection coefficient of the proposed antenna array (simulated values include substrate permittivity tolerance value).

realized expanded version of the proposed array in Fig. 6, where the array area has been doubled. Interestingly, the array looks from the top as a network of microstrip lines, and at the same time, they are acting in total as a radiating antenna. Fig. 11-a shows the realized gain and the total reflection coefficient of the array. A realized gain of 22.5 dBi is achieved. The 10 dB return loss matching bandwidth is 1.9 GHz (i.e., 3.2 % of relative bandwidth). A 1.7 % shift in the measured resonance frequency over the simulated resonance frequency is observed. This is attributed to the tolerance effects in the fabrication process, the copper roughness, and the fragile substrate small thickness. The sensitivity of the structure to such tolerance errors is noticeable at such high frequencies. To highlight that, when a different value of the dielectric constant of the substrate is varied by just 3.6% to be of the value of 2.28 instead of 2.2, the frequency shift disappears as shown in Fig. 11-b.

Fig. 12 shows the radiation pattern in the E- and H-plane. Low side-lobe and cross-polarization levels are obtained. The third side-lobe is a suppressed grating lobe.

Fig. 13 shows the calculated efficiency of the structure, excellent efficiency of 93% is achieved within the matching bandwidth.

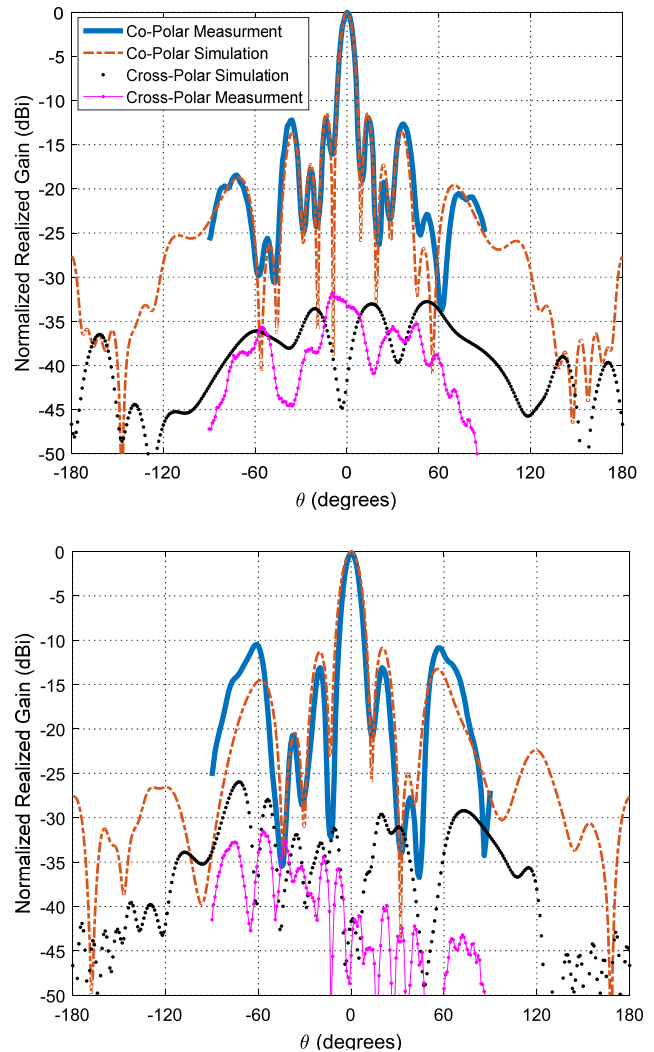


FIGURE 12. Radiation patterns of the proposed antenna array with aggregated microstrip feeding network, E-plane (top), and H-plane (bottom).

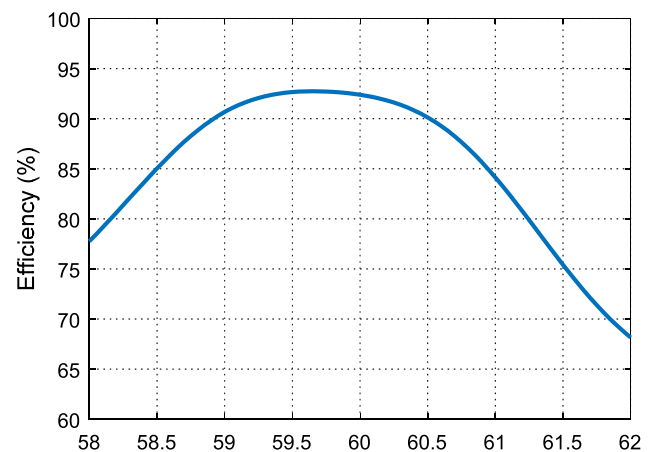


FIGURE 13. Radiation efficiency of the proposed antenna array.

Table 2 compares the proposed antenna array with others in the literature. As can be seen, the gain of the proposed antenna array is higher than any 4×4 antenna array, and this

TABLE 2. Comparison with other works.

Ref.	Freq. (GHz)	Array Type	Elements Number	BW (%)	Gain (dBi)
[4]	60	SIW Fed Slot Array	4x8	2	20.6
[5]	60	PCB Fringing Fields Ant.	1x4	11.6	16
[6]	60	PCB Monopoles	1x2	11.6	14
[7]	60	SIW Slot Antenna Array	12 x 12	4.17	22
[18]	60	Patch Antenna Array	4x4	11.6	18
[40]	60	SIW Slot Antenna Array	4 x 2	11.6	12
[41]	60	SIW Slot Antenna Array	8 x 8	17.1	22.1
[42]	60	Patch Antenna Array	4x4	9.5	18.2
[43]	60	Patch Antenna Array	4x4	28	16
[44]	60	SIW Slot antenna array	4x4	20.8	18.3
[45]	60	Microstrip Antenna Array	4x4	25.5	15.2
[46]	30	SIW Slot Antenna Array	4x4	8.5	19.1
[47]	45	Microstrip Antenna Array	4x4	24.4	18.8
[48]	30	SIW slot Antenna Array	4x4	4.6	16
[49]	60	Patch Antenna Array	4x4	18.3	17.5
[50]	60	Aperture Coupled Microstrip Ant. Array	6x8	1.8	21.6
[51]	24	Microstrip Antenna Array	8x8	4.1	18
This Work	60	Aggregated Fringing Fields Antenna Array	4x4	3.2	22.5

is the main merit of the proposed antenna in this work. As by the feed of only 4×4 elements, the gain of the antenna can be improved dramatically (since each element can be viewed as a sub-array of four magnetic current elements), and can compete with a higher number of elements arrays. This can be easily deduced by the fact that doubling the antenna array size would result in an ideally 3-dB increase in the gain. The bandwidth of the proposed antenna is limited to 3.2 % which is suitable for many millimeter wave applications. The physical dimension of the array is $28.95\text{mm} \times 19.3\text{mm}$, which is equivalent to $5.79\lambda_0 \times 3.86\lambda_0$, the calculated aperture efficiency is 76.3 %.

IV. CONCLUSION AND FUTURE WORK

A high gain antenna array has been designed and fabricated at 60 GHz. The array has been made on a single dielectric substrate with no vias, which contributed to its low cost. The array has achieved 22.5 dBi gain with a maximum efficiency of 93%, and 3.2 % bandwidth. The antenna structure is a suitable candidate to be integrated easily within any narrowband millimeter-wave transceiver system. A potential future works suggest the study of new techniques and methods to lower the quality factor and enhance the bandwidth of the proposed antenna array structure.

REFERENCES

- [1] F. A. Wyczalek, *Millimeter Wave Technology in Wireless PAN, LAN, and MAN*. New York, NY, USA: Auerbach, 2008.
- [2] D. Liu, B. Gaucher, U. Pfeiffer, and J. Grzyb, *Advanced Millimeter-wave Technologies: Antennas, Packaging and Circuits*. Chichester, U.K.: Wiley, 2009.
- [3] M. S. Sorkherizi, A. Dadgarpor, and A. A. Kishk, "Planar high-efficiency antenna array using new printed ridge gap waveguide technology," *IEEE Trans. Antennas Propag.*, vol. 65, no. 7, pp. 3772–3776, Jul. 2017.
- [4] H. Chu, J.-X. Chen, and Y.-X. Guo, "An efficient gain enhancement approach for 60-GHz antenna using fully integrated vertical metallic walls in LTCC," *IEEE Trans. Antennas Propag.*, vol. 64, no. 10, pp. 4513–4518, Oct. 2016.
- [5] Y. Al-Alem and A. A. Kishk, "Efficient millimeter-wave antenna based on the exploitation of microstrip line discontinuity radiation," *IEEE Trans. Antennas Propag.*, vol. 66, no. 6, pp. 2844–2852, Jun. 2018.
- [6] Y. Al-Alem and A. A. Kishk, "Low-profile low-cost high gain 60 GHz antenna," *IEEE Access*, vol. 6, pp. 13376–13384, 2018.
- [7] X.-P. Chen, K. Wu, L. Han, and F. He, "Low-cost high gain planar antenna array for 60-GHz band applications," *IEEE Trans. Antennas Propag.*, vol. 58, no. 6, pp. 2126–2129, Jun. 2010.
- [8] C. Kärmfelt, P. Hallbjörner, H. Zirath, and A. Alping, "High gain active microstrip antenna for 60-GHz WLAN/WPAN applications," *IEEE Trans. Microw. Theory Techn.*, vol. 54, no. 6, pp. 2593–2603, Jun. 2006.
- [9] X. Ruan, K. B. Ng, and C. H. Chan, "A differentially fed transmission-line-excited magnetolectric dipole antenna array for 5g applications," *IEEE Trans. Antennas Propag.*, vol. 66, no. 10, pp. 5224–5230, Oct. 2018.
- [10] Y. J. Cheng, *Substrate Integrated Antennas and Arrays*, 1st ed. Boca Raton, FL, USA: CRC Press, 2015.
- [11] K.-S. Chin, W. Jiang, W. Che, C.-C. Chang, and H. Jin, "Wideband LTCC 60-GHz antenna array with a dual-resonant slot and patch structure," *IEEE Trans. Antennas Propag.*, vol. 62, no. 1, pp. 174–182, Jan. 2014.
- [12] A. A. Qureshi, D. M. Klymyshyn, M. Tayfeh, W. Mazhar, M. Börner, and J. Mohr, "Template-based dielectric resonator antenna arrays for millimeter-wave applications," *IEEE Trans. Antennas Propag.*, vol. 65, no. 9, pp. 4576–4584, Sep. 2017.
- [13] M. Li and K.-M. Luk, "Wideband magneto-electric dipole antenna for 60-GHz millimeter-wave communications," *IEEE Trans. Antennas Propag.*, vol. 63, no. 7, pp. 3276–3279, Jul. 2015.
- [14] R. A. Alhalabi and G. M. Rebeiz, "Differentially-fed millimeter-wave Yagi-Uda antennas with folded dipole feed," *IEEE Trans. Antennas Propag.*, vol. 58, no. 3, pp. 966–969, Mar. 2010.
- [15] R. A. Alhalabi and G. M. Rebeiz, "High-efficiency angled-dipole antennas for millimeter-wave phased array applications," *IEEE Trans. Antennas Propag.*, vol. 56, no. 10, pp. 3136–3142, Oct. 2008.
- [16] Z. Chen, H. Liu, J. Yu, and X. Chen, "High gain, broadband and dual-polarized substrate integrated waveguide cavity-backed slot antenna array for 60 GHz band," *IEEE Access*, vol. 6, pp. 31012–31022, 2018.
- [17] J. Zhu, C.-H. Chu, L. Deng, C. Zhang, Y. Yang, and S. Li, "mm-Wave high gain cavity-backed aperture-coupled patch antenna array," *IEEE Access*, vol. 6, pp. 44050–44058, 2018.
- [18] S. B. Yeap, Z. N. Chen, and X. Qing, "Gain-enhanced 60-GHz LTCC antenna array with open air cavities," *IEEE Trans. Antennas Propag.*, vol. 59, no. 9, pp. 3470–3473, Sep. 2011.
- [19] J. Zhang, X. Zhang, and A. A. Kishk, "Broadband 60 GHz antennas fed by substrate integrated gap waveguides," *IEEE Trans. Antennas Propag.*, vol. 66, no. 7, pp. 3261–3270, Jul. 2018.
- [20] F.-J. Huang, C.-M. Lee, C.-Y. Kuo, and C.-H. Luo, "MMW antenna in IPD process for 60-GHz WPAN applications," *IEEE Antennas Wireless Propag. Lett.*, vol. 10, pp. 565–568, 2011.
- [21] M. Sun, X. Qing, and Z. N. Chen, "60-GHz end-fire fan-like antennas with wide beamwidth," *IEEE Trans. Antennas Propag.*, vol. 61, no. 4, pp. 1616–1622, Apr. 2013.
- [22] P.-S. Kildal, *Foundations of Antenna Engineering: A Unified Approach for Line-of-Sight and Multipath*. Norwood, MA, USA: Artech House, 2015.
- [23] Y. T. Lo and S. W. Lee, Eds., *Antenna Handbook: Theory, Applications, and Design*. Boston, MA, USA: Springer, 1988.
- [24] Z.-G. Liu, "Fabry-Perot Resonator antenna," *J. Infr., Millim., Terahertz Waves*, vol. 31, no. 4, pp. 391–403, 2010.
- [25] H. Attia, L. Yousefi, and O. Ramahi, "High gain microstrip antennas loaded with high characteristic impedance superstrates," in *Proc. IEEE Int. Symp. Antennas Propag. (APSURSI)*, Jul. 2011, pp. 1258–1261.
- [26] H. Attia, M. L. Abdelghani, and T. A. Denidni, "Wideband and high-gain millimeter-wave antenna based on FSS Fabry-Perot cavity," *IEEE Trans. Antennas Propag.*, vol. 65, no. 10, pp. 5589–5594, Oct. 2017.
- [27] R. M. Hashmi, B. A. Zeb, and K. P. Esselle, "Wideband high-gain EBG resonator antennas with small footprints and all-dielectric superstructures," *IEEE Trans. Antennas Propag.*, vol. 62, no. 6, pp. 2970–2977, Jun. 2014.
- [28] M. Asaadi and A. Sebak, "Gain and bandwidth enhancement of 2×2 square dense dielectric patch antenna array using a holey superstrate," *IEEE Antennas Wireless Propag. Lett.*, vol. 16, pp. 1808–1811, 2017.
- [29] H. Attia, M. S. Sorkherizi, and A. A. Kishk, "60 GHz slot antenna array based on ridge gap waveguide technology enhanced with dielectric superstrate," in *Proc. 9th Eur. Conf. Antennas Propag. (EuCAP)*, Apr. 2015, pp. 1–4.
- [30] A. A. Kishk, "One-dimensional electromagnetic bandgap for directivity enhancement of waveguide antennas," *Microw. Opt. Technol. Lett.*, vol. 47, no. 5, pp. 430–434, 2005.
- [31] H. Attia, M. S. Sorkherizi, and A. A. Kishk, "Reduction of grating lobes for slot antenna array at 60 GHz using multilayer spatial angular filter," in *Proc. IEEE Int. Symp. Antennas Propag. USNC/URSI Nat. Radio Sci. Meeting*, Jul. 2015, pp. 2043–2044.
- [32] M. Al Sharkawy and A. A. Kishk, "Split slots array for grating lobe suppression in ridge gap guide," *IEEE Antennas Wireless Propag. Lett.*, vol. 15, pp. 946–949, 2015.

- [33] A. A. Kishk, "Enhanced gain of scanning DRA array," in *Proc. 10th Eur. Conf. Antennas Propag. (EuCAP)*, Apr. 2016, pp. 1–3.
- [34] A. A. Kishk and L. Shafai, "Gain enhancement of antennas over finite ground plane covered by a dielectric sheet," *IEE Proc. H-Microw., Antennas Propag.*, vol. 134, no. 1, pp. 60–64, Feb. 1987.
- [35] M. S. Sorkherizi and A. A. Kishk, "Fully printed gap waveguide with facilitated design properties," *IEEE Microw. Wireless Compon. Lett.*, vol. 26, no. 9, pp. 657–659, Sep. 2016.
- [36] D. Sievenpiper, "High-impedance electromagnetic surfaces," Univ. California, Berkeley, Berkeley, CA, USA, 1999.
- [37] E. Pucci, E. Rajo-Iglesias, J.-L. Vázquez-Roy, and P.-S. Kildal, "Planar dual-mode horn array with corporate-feed network in inverted microstrip gap waveguide," *IEEE Trans. Antennas Propag.*, vol. 62, no. 7, pp. 3534–3542, Jul. 2014.
- [38] T. A. Milligan, *Modern Antenna Handbook*. Hoboken, NJ, USA: Wiley, 2008.
- [39] C. A. Balanis, Ed., *Modern Antenna Handbook*, 1st ed. Hoboken, NJ, USA: Wiley, 2008.
- [40] K. Gong, Z. N. Chen, X. Qing, P. Chen, and W. Hong, "Substrate integrated waveguide cavity-backed wide slot antenna for 60-GHz Bands," *IEEE Trans. Antennas Propag.*, vol. 60, no. 12, pp. 6023–6026, Dec. 2012.
- [41] J. Xu, Z. N. Chen, X. Qing, and W. Hong, "Bandwidth enhancement for a 60 GHz substrate integrated waveguide fed cavity array antenna on LTCC," *IEEE Trans. Antennas Propag.*, vol. 59, no. 3, pp. 826–832, Mar. 2011.
- [42] A. E. I. Lamminen, J. Saily, and A. R. Vimpari, "60-GHz patch antennas and arrays on LTCC with embedded-cavity substrates," *IEEE Trans. Antennas Propag.*, vol. 56, no. 9, pp. 2865–2874, Sep. 2008.
- [43] H. Sun, Y.-X. Guo, and Z. Wang, "60-GHz circularly polarized u-slot patch antenna array on LTCC," *IEEE Trans. Antennas Propag.*, vol. 61, no. 1, pp. 430–435, Jan. 2013.
- [44] S. Liao, P. Chen, P. Wu, K. M. Shum, and Q. Xue, "Substrate-integrated waveguide-based 60-GHz resonant slotted waveguide arrays with wide impedance bandwidth and high gain," *IEEE Trans. Antennas Propag.*, vol. 63, no. 7, pp. 2922–2931, Jul. 2015.
- [45] M. Li and K.-M. Luk, "Low-cost wideband microstrip antenna array for 60-GHz applications," *IEEE Trans. Antennas Propag.*, vol. 62, no. 6, pp. 3012–3018, Jun. 2014.
- [46] H. Jin, W. Che, K.-S. Chin, W. Yang, and Q. Xue, "Millimeter-wave TE₂₀-mode SIW dual-slot-fed patch antenna array with a compact differential feeding network," *IEEE Trans. Antennas Propag.*, vol. 66, no. 1, pp. 456–461, Jan. 2018.
- [47] Z. Gan, Z.-H. Tu, Z.-M. Xie, Q.-X. Chu, and Y. Yao, "Compact wideband circularly polarized microstrip antenna array for 45 GHz application," *IEEE Trans. Antennas Propag.*, vol. 66, no. 11, pp. 6388–6392, Nov. 2018.
- [48] M. Asaadi and A. Sebak, "High-gain low-profile circularly polarized slotted SIW cavity antenna for MMW applications," *IEEE Antennas Wireless Propag. Lett.*, vol. 16, pp. 752–755, 2016.
- [49] L. Wang, Y.-X. Guo, and W.-X. Sheng, "Wideband high-gain 60-GHz LTCC L-probe patch antenna array with a soft surface," *IEEE Trans. Antennas Propag.*, vol. 61, no. 4, pp. 1802–1809, Apr. 2013.
- [50] T. Mikulasek, J. Lacik, J. Puskely, and Z. Raida, "Design of aperture-coupled microstrip patch antenna array fed by SIW for 60 GHz band," *IET Microw., Antennas Propag.*, vol. 10, no. 3, pp. 288–292, Feb. 2016.
- [51] K. Wincza and S. Gruszczynski, "Microstrip antenna arrays fed by a series-parallel slot-coupled feeding network," *IEEE Antennas Wireless Propag. Lett.*, vol. 10, pp. 991–994, 2011.



YAZAN AL-ALEM received the B.Sc. degree in electrical engineering from The University of Jordan, in 2010, and the M.Sc. degree in electrical engineering from the American University of Sharjah, in 2015. He is currently pursuing the Ph.D. degree with Concordia University, Montreal, QC, Canada. He received the Concordia University International Tuition Award of Excellence and the American University of Sharjah Full Graduate Teaching and Research Assistantship.



AHMED A. KISHK received the B.S. degree in electronic and communication engineering from Cairo University, Cairo, Egypt, in 1977, and the B.Sc. degree in applied mathematics from Ain Shams University, Cairo, in 1980, and the M.Eng. and Ph.D. degrees from the Department of Electrical Engineering, University of Manitoba, Winnipeg, MB, Canada, in 1983 and 1986, respectively. In 1986, he joined the Department of Electrical Engineering, University of Mississippi.

He was a Professor with the University of Mississippi, from 1995 to 2011. He is currently a Professor with Concordia University, Montreal, QC, Canada, (since 2011) as Tier 1 Canada Research Chair in Advanced Antenna Systems. He was the 2017 AP-S President.

He has published over 320 refereed journal articles and 450 conference papers. He has co-authored four books and several book chapters and the Editor of three books. His research interests include the areas of millimeter wave antennas for 5G applications, analog beamforming networks, antennas, microwave passive circuits and components, EBG, artificial magnetic conductors, phased array antennas, reflect/transmitarray, and wearable antennas.

• • •